



Hybrid COOT-ANN: a novel optimization algorithm for prediction of daily crop reference evapotranspiration in Australia

Ehsan Mirzania¹ · Mahsa Hasanpour Kashani² · Golmar Golmohammadi³ · Osama Ragab Ibrahim⁴ · Mohsen Saroughi⁵

Received: 22 November 2022 / Accepted: 23 June 2023 / Published online: 4 July 2023
© The Author(s), under exclusive licence to Springer-Verlag GmbH Austria, part of Springer Nature 2023

Abstract

The present study evaluates the capability of a novel optimization method in modeling daily crop reference evapotranspiration (ET_0), a critical issue in water resource management. A hybrid predictive model based on the artificial neural network (ANN) algorithm that is embedded within the COOT method (COOT bird natural life model-artificial neural network (COOT-ANN)) is developed and evaluated for its suitability for the prediction of daily ET_0 at seven meteorological stations in different states of Australia. Accordingly, a daily statistical period of 12 years (01-01-2010 to 31-12-2021) for climatic data of maximum temperature, minimum temperature, and ET_0 were collected. The results are evaluated using six performance criteria metrics: correlation coefficient (R), root mean square error (RMSE), Nash–Sutcliffe efficiency (NSE), RMSE-observation standard deviation ratio (RSR), Scatter Index (SI), and mean absolute error (MAE) along with the Taylor diagrams. The performance of the COOT-ANN model was compared with those of the conventional ANN model. The results showed that the COOT-ANN hybrid model outperforms the ANN model at all seven stations by 0.803%, 4.127%, 3.359%, 4.072%, 4.148%, and 3.665% based on the average values of the R , RMSE, NSE, RSR, SI, and MAE criteria, respectively. So, this study provides an innovative method for prediction in agricultural and water resource studies.

✉ Ehsan Mirzania
e.mirzania99@ms.tabrizu.ac.ir

✉ Mohsen Saroughi
mohsensaroughi@ut.ac.ir

Mahsa Hasanpour Kashani
m.hkashani@uma.ac.ir

Golmar Golmohammadi
g.golmohammadi@ufl.edu

Osama Ragab Ibrahim
oibrahim@su.edu.om

¹ Department of Water Engineering, University of Tabriz, Tabriz, Iran

² Department of Water Engineering, Water Management Research Center, Faculty of Agriculture and Natural Resources, University of Mohaghegh Ardabili, Ardabil, Iran

³ Department of Soil, Water and Ecosystem Sciences, University of Florida, Gainesville, FL, USA

⁴ Department of Civil Engineering, Faculty of Engineering, Sohar University, Sohar, Oman

⁵ Department of Irrigation and Reclamation Engineering, Faculty of Agricultural Engineering and Technology, College of Agriculture and Natural Resources, University of Tehran, Karaj, Iran

1 Introduction

Crop reference evapotranspiration (ET_0), a vital element in the hydrological cycle, plays a significant role in the effective use of existing water resources and planning sustainable water management. An immediate and certain consequence of global warming is an increase in temperature (Salman et al. 2017; Pour et al. 2019). Increasing temperature will alter ET_0 , which will have significant impacts on water resources. For water resource management, planning, and development, accurate estimation of ET_0 has become crucial due to the global warming and climate change impact studies (Muhammad et al. 2021). It is vitally important for agriculture and irrigation to estimate the amount of evapotranspiration. An incorrect measurement of evapotranspiration may lead to excessive plant water requirements, nutrient leaching, and groundwater pollution (Kisi et al. 2021). Several meteorological variables including global solar radiation (R_s), ambient temperature (T_{max} and T_{min}), relative humidity (RH), and wind speed (U_2) influence the evapotranspiration process. Huang et al. (2019) predicted ET_0 using meteorological variables of maximum temperature (T_{max}), minimum temperature (T_{min}), relative humidity (RH),

wind speed (U), and solar radiation (R_s). Majhi and Naidu (2021) estimated ET_o using data of maximum temperature (T_{max}), minimum temperature (T_{min}), sunshine hours (SH), minimum wind speed (U_{min}), relative humidity (RH), and cumulative pan evaporation (Ep). Maroufpoor et al. (2020) used maximum temperature (T_{max}), minimum temperature (T_{min}), relative humidity (RH), sunshine hours (SH), average wind speed (U_{mean}), and precipitation (P) to estimate ET_o . The FAO-56 PM model which has been used in many areas to estimate ET_o , however, is limited by the fact that it requires many climatic variables. The required instruments for this model can be difficult and expensive to install and maintain (Exner-Kittridge and Rains 2010; Valiantzas 2015). Therefore, this model is rarely used especially in developed countries (Shiri 2017; Yamaç and Todorovic 2020; Koudahe et al. 2018; Djaman et al. 2019).

The ET_o of plants can be determined by equations like FAO Penman, FAO Penman–Monteith, and Blaney–Criddle (Feng et al. 2017; Chen et al. 2019a, 2019b). Even though these methods perform well in most cases, they cannot handle nonlinear complexities well and require a vast amount of input data, which may not always be available. In recent years, artificial intelligence (AI) and soft computing techniques have gained significant attention in a variety of engineering and medical fields. A literature review of time series, empirical, and data-driven modeling techniques was conducted to simulate ET_o (Huang et al. 2019; Fan et al. 2018; Nourani et al. 2019; Yu et al. 2020; Sharafi and Ghalehi 2021; Douna et al. 2021; Keshtegar et al. 2022; Mirzania et al. 2023; Majumdar et al. 2023). There have already been several conventional artificial neural network (ANN) algorithm modeling techniques that have proven to be successful in modeling ET_o (Achite et al. 2022; Gocić and Amiri 2021; Nawandar et al. 2021; Abrishami et al. 2019; Hashemi and Sepaskhah 2020). Antonopoulos and Antonopoulos (2017) predicted daily ET_o in northern Greece and found that the ANN model has a more accurate prediction than other models. Ferreira et al. (2019) investigated the performance of ANN and support vector machine (SVM) models in estimating daily ET_o in Brazil and concluded that the results of the ANN model are better than the other one.

According to a recent study, Elbeltagi et al. (2022) modeled the ET_o in Ludhiana (i.e., sub-humid climate) located in Northern India using five hybrid ANN-based models including artificial neural networks-additive regression (ANN-AR), ANN-random forest (ANN-RF), ANN-REP-tree, ANN-M5Pruning tree (ANN-M5P), and ANN-bagging models. Finally, the ANN-M5P model was selected as the best model based on the performance criteria values of MAE = 0.730 mm/day, RMSE = 0.959 mm/day, NSE = 0.779, and WI = 0.935. Maroufpoor et al. (2020) estimated ET_o using the standalone ANN model, hybrid artificial neural

network-gray wolf optimization (ANN-GWO) model, and least square support vector regression (LS-SVR) models in Iran. Finally, the hybrid ANN-GWO model was selected as the best model with the values of MAE = 0.279, SI = 0.077, and $R^2 = 0.981$ at the testing phase.

Ahmed et al. (2022) used the convolutional neural networks and gated recurrent unit (CNN-GRU) model to predict ET_o for a week ahead and obtained $R = 0.993$ and RMSE = 0.087 for the superior model at the validation stage. Zhao et al. (2019) applied a set of global climate models (GCMs) to determine ET_o at the seasonal and monthly scales. The COOT-ANN hybrid model has not been used to estimate ET_o in Australia.

In the field of crop reference evapotranspiration, several studies have been conducted using machine learning (ML) techniques (Mokari et al. 2021; Kaya et al. 2021; Niaghi et al. 2021; Dias et al. 2021; Chen et al. 2020; Üneş et al. 2020; Farias et al. 2020). New algorithms are being developed globally to improve accuracy, reduce errors, and lower costs. Consequently, many researchers employ such algorithms when developing models in a variety of fields. These researchers strive to measure the efficiency and effectiveness of their models on an industrial and global scale.

In recent years, the hybrid intelligent models have been developed to enhance the performance of the standalone AI models. Bio-inspired optimization algorithms draw significant attention for developing hybrid models in hydrological studies like estimating ET_o (Ahmadi et al. 2021). Seifi and Riahi (2020) proposed three hybrid models, namely, least square support vector machine-gamma test (LSSVM-GT), artificial neural network-gamma test (ANN-GT), and adaptive neuro fuzzy inference system-gamma test (ANFIS-GT) for predicting daily ET_o at arid areas of Iran. The results of this study showed that the hybrid LSSVM-GT model provides higher accuracy than the others. Maroufpoor et al. (2020) estimated evapotranspiration using ANN, artificial neural network-gray wolf optimization (ANN-GWO), and least square support vector regression (LS-SVR) models in Iran; the result showed the high ability of the ANN-GWO model than ANN and LS-SVR models. Gao et al. (2021) used three hybrid models, namely, artificial neural network-bat algorithm (BA-ANN), Cuckoo Search algorithm-artificial neural network (CSA-ANN), and whale optimization algorithm (WOA-ANN) to model daily ET_o with limited inputs and found that the hybrid WOA-ANN generated better estimations than the BA-ANN and CSA-ANN. Yang et al. (2022) showed that a calibrating anomaly improves daily reference crop evapotranspiration forecasts with two models Australian Community Climate and Earth-System Simulator G2 version (ACCESS-G2) and Seasonally Coherent Calibration (SCC) in Australia.

The Coot bird natural life model (COOT) algorithm is an innovative algorithm, which has not been used in

hydrological problems; however, it has successfully been used in other different fields. Mawgoud et al. (2022) investigated an effective hybrid approach based on the arithmetic optimization algorithm and sine cosine algorithm for the integration of battery energy storage system in distribution networks by the (COOT). They have used various models such as sine–cosine approach (SCA), arithmetic optimization algorithm (AOA), dynamic programming (DP), and coupled models of arithmetic optimization algorithm–sine cosine approach (AOA-SCA) models. Mostafa et al. (2022) used the modified COOT algorithm (mCOOT) based on two techniques opposition-based learning (OBL) and orthogonal learning for dimensionality reduction.

In this study, the COOT algorithm was used to improve the accuracy and effectiveness of artificial neural networks. Although hybrid models may be able to perform better than single models, it is usually an exchange between the training time and the performance of the model. In this study, to enhance the efficiency and easier training of the model, a hybrid predictive model based on the ANN algorithm and the COOT method (COOT-ANN) was developed. The developed hybrid COOT-ANN model would help to resolve some weaknesses of ANN, such as being trapped in local optimal solutions, which could result in higher accuracy and lower error rates.

According to the author's best knowledge, there are no studies on the application of hybrid COOT-ANN model in water resource fields. The purpose of this study is to develop and evaluate the performance of the hybrid COOT-ANN model in predicting ET_o and to compare its performance with the standalone intelligent ANN model. In this research,

a novel hybrid model was developed and used to predict ET_o in various climate stations in Australia. The results were compared with a simple machine learning model which has been used previously to predict ET_o in a single station or climate. This research makes an important contribution to assessing crop reference evapotranspiration under different climates. The findings of the present study could help in recommendations for modeling crop reference evapotranspiration in different climate in Australia. to planning sustainable water resources management.

2 Materials and methods

2.1 Case study and data used

Data required for this research include daily minimum and maximum temperatures (T_{\min} ($^{\circ}\text{C}$), T_{\max} ($^{\circ}\text{C}$)) and crop reference evapotranspiration (ET_o (mm/day)) which were collected from January 1, 2010, to December 31, 2021, from seven meteorological sites in Australia. The temperature data were obtained from the Australian Meteorological Agency (BOM) (<http://www.bom.gov.au>), while the ET_o data were obtained from both meteorological station records and satellite measurements. Seven meteorological stations in seven different states of Australia, namely, Leinster Aero, Charleville Aero, Stawell Aerodrome, Tennant Creek Airport, Woomera Aerodrome, Butlers Gorge, and Mudgee Airport, were used in this study (Fig. 1). The stations with complete data and no missing or noisy data were selected. The information related to each station is presented in Table 1. Table 2

Fig. 1 Location of the meteorological stations in seven states in Australia

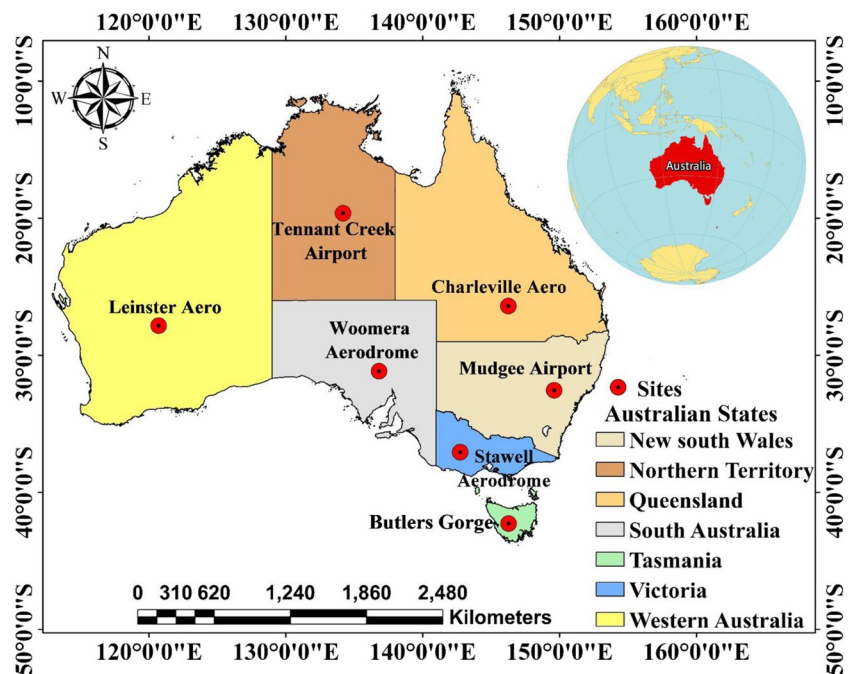


Table 1 Characteristics of the stations

Number	Station	State	Latitude (decimal)	Longitude (decimal)	Elevation (m)
1	Leinster Aero	Western Australia	-27.84	120.7	497
2	Charleville Aero	Queensland	-26.41	146.26	301.6
3	Stawell Aerodrome	Victoria	-37.07	142.74	235.36
4	Tennant Creek Airport	Northern Territory	-19.64	134.18	375.7
5	Woomera Aerodrome	South Australia	-31.16	136.81	166.6
6	Butlers Gorge	Tasmania	-42.28	146.28	667
7	Mudgee Airport	New south Wales	-32.56	149.61	471

Table 2 Statistical characteristics of the meteorological data

Parameter	Station	Min	Max	Mean	Std.	C.v.	Skew	Kurtosis
Maximum temperature (°C)	Leinster Aero	9.700	47.800	28.661	7.736	0.270	0.010	-0.981
	Charleville Aero	8.100	46.100	29.112	6.790	0.233	-0.126	-0.818
	Stawell Aerodrome	7.200	44.700	20.512	7.423	0.362	0.617	-0.437
	Tennant Creek Airport	10.400	45.600	32.520	5.803	0.178	-0.389	-0.610
	Woomera Aerodrome	8.500	48.200	26.682	7.839	0.294	0.296	-0.844
	Butlers Gorge	1.000	33.800	13.425	5.878	0.438	0.690	-0.089
	Mudgee Airport	5.700	43.900	23.066	6.921	0.300	0.249	-0.683
Minimum temperature (°C)	Leinster Aero	0.000	32.600	14.875	6.954	0.467	-0.056	-0.943
	Charleville Aero	0.000	31.200	14.565	7.325	0.503	-0.178	-1.002
	Stawell Aerodrome	0.000	26.900	8.920	4.567	0.512	0.485	0.144
	Tennant Creek Airport	5.700	33.100	20.067	5.447	0.271	-0.412	-0.811
	Woomera Aerodrome	0.700	32.300	13.192	6.205	0.470	0.269	-0.701
	Butlers Gorge	0.000	19.400	4.615	2.891	0.626	0.939	1.129
	Mudgee Airport	0.000	26.000	9.851	5.490	0.557	0.192	-0.822
ET _o (mm/day)	Leinster Aero	0.700	15.400	6.293	2.983	0.474	0.276	-0.950
	Charleville Aero	0.700	13.700	5.614	2.562	0.456	0.344	-0.862
	Stawell Aerodrome	0.400	13.900	3.681	2.408	0.654	0.722	-0.232
	Tennant Creek Airport	0.900	14.800	7.548	2.153	0.285	0.137	-0.347
	Woomera Aerodrome	0.800	19.800	6.360	3.269	0.514	0.455	-0.509
	Butlers Gorge	0.100	7.900	2.073	1.488	0.718	0.914	0.036
	Mudgee Airport	0.400	13.400	3.898	2.198	0.564	0.604	-0.482

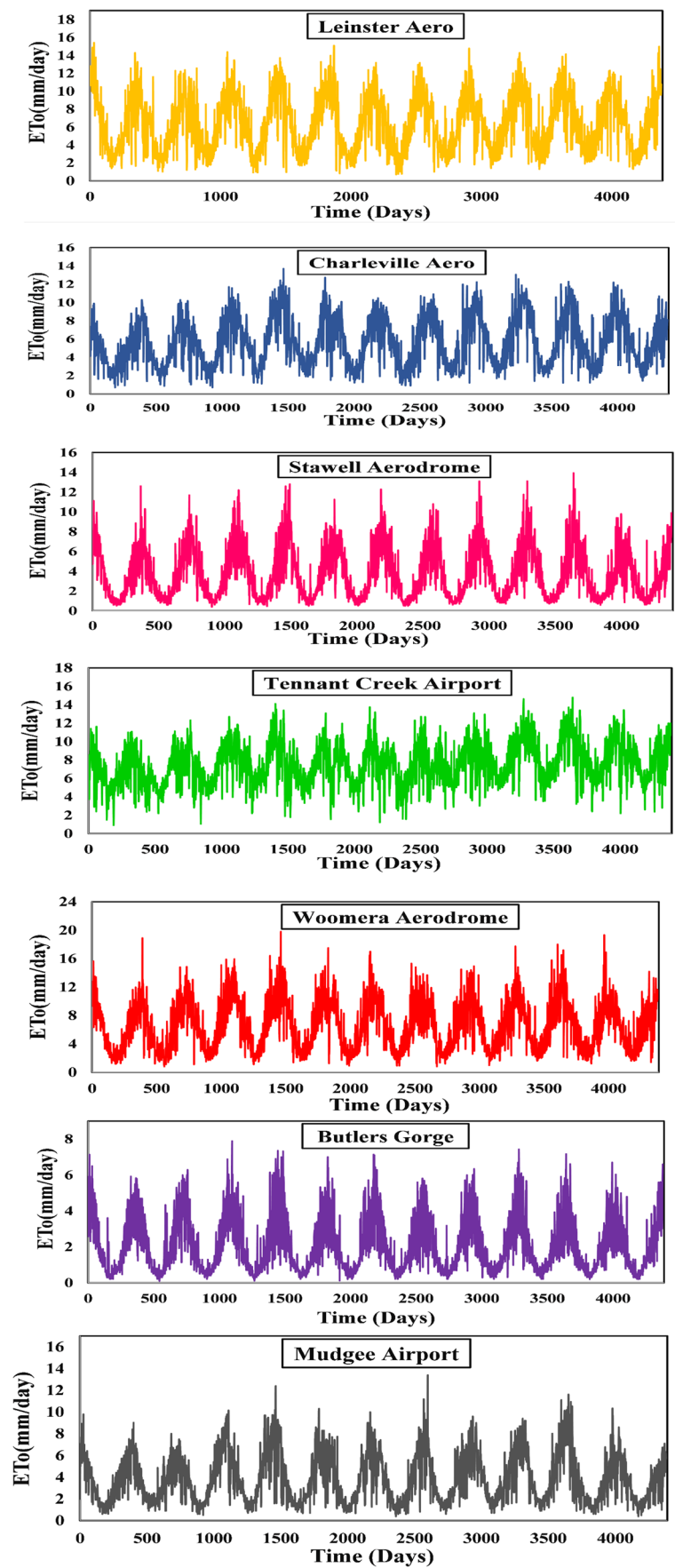
shows the statistical characteristics of the daily meteorological data in different stations. For training and testing of the models, 80% and 20% of daily data were used, respectively. A time series diagram of the observed daily ET_o data for the selected stations is presented in Fig. 2. The time series plot of crop reference evapotranspiration for seven stations (Fig. 2) indicates that the Butlers Gorge station has the lowest crop reference evapotranspiration rate and the Tennant Creek Airport station has the highest crop reference evapotranspiration rate. Australia is a large continent in the Oceania region spanning 35° of latitude and, as such, has several climate zones. Australia's northern regions have a tropical climate and large amounts of evapotranspiration are caused by the hot, humid weather. In contrast, in the southern part, there are distinct seasons with dry summers and wet winters;

coastal areas also tend to have a low evapotranspiration rate due to their proximity to large water sources.

2.2 Artificial neural network

The function of an ANN is to receive, process, and generate information much like that of biological neuronal networks. In ANNs, repetition is the key to learning. When different data is entered into the learning algorithm numerous times, the difference in the amount of data can be detected by the changes that occur in the weight and bias vectors. The back-propagation of error, also called back propagation (BP), is one of the most widely used methods for training the ANN. In this algorithm, each iteration involves two steps: the first step is a feed-forward motion, which multiplies inputs with weights and sums

Fig. 2 Observed daily crop reference evapotranspiration time series at the studied stations (2010–2021)



them with bias vectors. Feed-forward motion involves measuring the error values after obtaining the output values and comparing them with the targets. So, by finding out about error values related to the weights and biases, the algorithm moves on to the next step, which is back-propagation, and modifies the parameters based on the error values. Iterations (feed-forward and back-propagation) are performed until the predicted output is very close to the desired output (target). In order to get a better cost function topology, it is better to scale the data into the given interval before training an ANN model. An optimization algorithm may not be able to find the optimal values if the data is not scaled into the given scale. A network can learn optimal parameters more quickly when data is scaled within a given interval (Nourani 2017).

2.3 Coot bird natural life model

The Coot bird natural life model (COOT) algorithm simulated the different collective behaviors of Coots, a small water bird in the rail family, using a metaheuristic optimization algorithm. On the surface of the water, coots make regular and irregular movements; this behavior is ultimately aimed at moving towards food or to a specific location (Naruei and Keynia 2021). Four different movement patterns can be observed on the water surface of a coot group: random movement, chain movement, adjusting position according to leader, and leader movement (Naruei and Keynia 2021). The COOT algorithm is implemented using these four movements' behaviors. The specific implementation procedure is as follows (Naruei and Keynia 2021): creation of the population is randomly initialized by according to Eq. (1):

$$\text{CootPos}(i) = \text{rand}(1, d) \times (\text{ub} - \text{lb}) + \text{lb} \quad (1)$$

where $\text{CootPos}(i)$ represents the position of the coot, d is the number of variables or dimensions of the problem, ub and lb represent the upper and the lower bound of the search space, respectively.

$$\text{ub} = [\text{ub}_1, \text{ub}_2, \dots, \text{ub}_d], \text{lb} = [\text{lb}_1, \text{lb}_2, \dots, \text{lb}_d] \quad (2)$$

Following the initialization of the population, the coot's position is updated according to four movement patterns.

2.3.1 Random movement

The position Q for this movement is first randomly initialized by using Eq. (3):

$$Q = \text{rand}(1, d) \times (\text{ub} - \text{lb}) + \text{lb} \quad (3)$$

The position is updated according to Eq. (4) in order to avoid being trapped in a local optimum:

$$\text{CootPos}(i) = \text{CootPos}(i) + A \times R_2 \times (Q - \text{CootPos}(i)) \quad (4)$$

where R_2 is a random number in the interval $[0, 1]$, and A is calculated as Eq. (5):

$$A = 1 - L \times \left(\frac{1}{\text{Iter}} \right) \quad (5)$$

where Iter is the maximum number of iterations and L is the current number of iterations.

2.3.2 Chain movement

In order to implement the chain movement, the average position of the two coot birds can be calculated using Eq. (6):

$$\text{CootPos}(i) = \frac{\text{CootPos}(i-1) + \text{CootPos}(i)}{2} \quad (6)$$

In this case, $\text{CootPos}(i-1)$ indicates the location of the second coot.

2.3.3 Adjusting position according to the leader

During each group, a coot bird's position updates based on the position of the leader; therefore, the follower moves towards the leader. The leader is selected using Eq. (7):

$$K = 1 + (i \text{ MOD } \text{NL}) \quad (7)$$

where K is represented as the number of the leader index, i is the number of the coot bird follower, and NL is the number of leaders.

A coot's position is updated according to Eq. (8) during this movement:

$$\text{CootPos}(i) = \text{LeaderPos}(k) + 2 \times R_1 \times \text{Cos}(2\pi R) \times (\text{LeaderPos}(k) - \text{CootPos}(i)) \quad (8)$$

Using $\text{CootPos}(i)$ as the current position of the coot bird, the $\text{LeaderPos}(k)$ represents the position of the selected leader, R_1 is a random number in the interval $[0, 1]$, and R is a random number in the interval $[-1, 1]$.

2.3.4 Leader movement

Leader positions are updated using Eq. (9) based on the leap from local optimal positions to global optimal positions:

$$\text{LeaderPos}(i) = \begin{cases} B \times B_3 \times \text{Cos}(2\pi R) \times (g\text{Best} - \text{LeaderPos}(i)) + g\text{Best} & R_4 < 0.5 \\ B \times B_3 \times \text{Cos}(2\pi R) \times (g\text{Best} - \text{LeaderPos}(i)) + g\text{Best} & R_4 \geq 0.5 \end{cases} \quad (9)$$

where g_{Best} refers to the best position that can be found, $R3$ and $R4$ are the random numbers between the interval $[0, 1]$, and R is the random number between the interval $[-1, 1]$. B is determined from Eq. (10):

$$B = 2 - L \times \left(\frac{1}{Iter} \right) \tag{10}$$

2.4 Hybrid model (COOT-ANN)

In the COOT-ANN model, the optimization COOT algorithm is applied to determine the best and optimum values of the ANN's parameters and so increase its ability in accurately predicting different problems. Hybrid algorithms have many advantages, including their flexibility of implementation, unconditional formulation of problems, and absence of derivatives. When a mathematical function reaches certain fitness between COOT and ANN, then hybrid models (i.e., COOT-ANN) stop, or when iterations reach the maximum number, then the model stops. This approach allows the models to reach their maximum capabilities, and then the new hybrid model can have advantages of the ANN and optimization (Mohammadi et al. 2020). Table 3 shows the parameters used in the modeling process. Figure 3 illustrates a flowchart of the COOT-ANN model used throughout the research. Figure 3 presents a summary of the COOT-ANN hybrid algorithm; it depicts how the hybrid algorithm process involves the combining of two or more algorithms to solve a particular problem, with the goal of setting the optimal parameters to reduce error and improve accuracy. Figure 4 presents the Pseudo code of the COOT algorithm and an overview of parameters which has been used and updated, as well as the performance of the COOT algorithm with the best configuration during learning process.

2.5 Performance evaluation statistics

The predictive models are evaluated using six performance criteria, namely, correlation coefficient (R), root mean

squared error (RMSE), Nash-Sutcliffe efficiency (NSE), RMSE-observation standard deviation ratio (RSR), Scatter Index (SI), and mean absolute error (MAE):

Correlation coefficient (R)

$$R = \frac{\sum_{i=1}^N (EO - \overline{EO})(EP - \overline{EP})}{\sqrt{\sum_{i=1}^N (EO - \overline{EO})^2 \cdot \sum_{i=1}^N (EP - \overline{EP})^2}} - 1 \leq R \leq 1 \tag{11}$$

Root mean square error (RMSE)

$$RMSE = \sqrt{\frac{1}{N} \sum_{i=1}^N (EP - EO)^2} \quad 0 \leq RMSE \leq \infty \tag{12}$$

Nash-Sutcliffe Efficiency Coefficient (NSE)

$$NSE = 1 - \left[\frac{\sum_{i=1}^N (EO - EP)^2}{\sum_{i=1}^N (EO - \overline{EO})^2} \right] - \infty < NSE \leq 1 \tag{13}$$

RMSE-observation standard deviation ratio (RSR)

$$RSR = \frac{\sqrt{\sum_{i=1}^N (EO - EP)^2}}{\sqrt{\sum_{i=1}^N (EO - \overline{EO})^2}} \quad 0 \leq RSR \leq \infty \tag{14}$$

Scatter Index (SI)

$$SI = \frac{\sqrt{\frac{1}{N} \sum_{i=1}^N (EP - EO)^2}}{\overline{EO}} \quad 0 \leq SI \leq \infty \tag{15}$$

Mean absolute error (MAE)

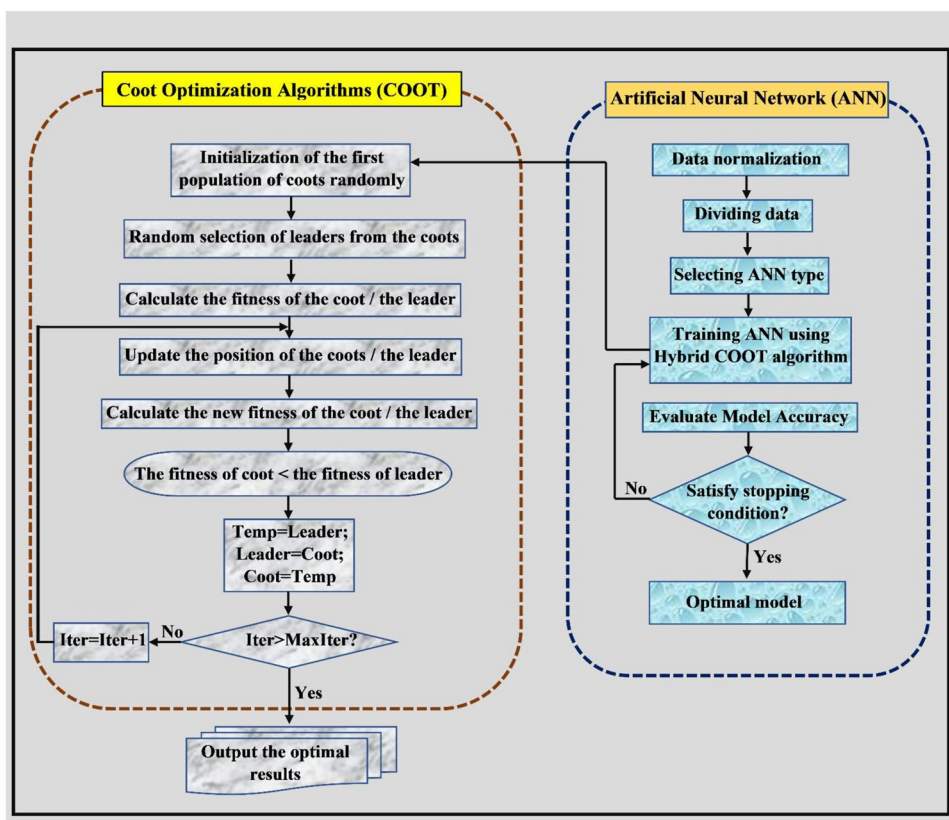
$$MAE = \frac{1}{N} \sum_{i=1}^N (EP - EO) \quad 0 \leq MAE \leq \infty \tag{16}$$

where EO and EP are the observed and predicted ET_o values, N denotes the number of observations, and \overline{EO} and \overline{EP}

Table 3 Parameters used for training the ANN and COOT-ANN models

Model		COOT-ANN	
Model parameter	Value/type	Model parameter	Value
ANN		COOT-ANN	
Network type	Feed-forward back propagation	Maxiter	1000
Number of hidden layers (neurons)	10	Pop size	500
Data division	dividerand	Number of hidden layers (neurons)	10
Training function	adam	Learning rate	0.001
Transfer function layer1	relu	P	0.1
Epoch	1000	NL	50
		NC	450

Fig. 3 Flowchart of the COOT-ANN model



are the means of the observed and predicted ET_0 . Table 4 indicates classification of a model's performance based on the NSE and RSR criteria values.

3 Application and results

In order to achieve an optimal model in a data-driven modeling approach, input variables are being fed into the models one by one. In this study, daily T_{\max} ($^{\circ}C$) and T_{\min} ($^{\circ}C$) variables in all the stations were used as the inputs of the classical ANN and hybrid COOT-ANN models. Initially, the back propagation feed forward algorithm was used in the classical ANN model, while in the second step, the Coot bird natural life algorithm was coupled with ANN to increase the model's preciseness. Figure 5 illustrates a summary of the methodology used in this study. The performance of developed models was evaluated by the Taylor diagrams and the statistical metrics including R , RMSE, NSE, RSR, SI, and MAE. Table 5 shows the models' performance based on the six statistical measures in the training and test periods for all the seven stations for ANN and COOT-ANN models.

The statistical analysis shows that the COOT-ANN model is able to predict the daily ET_0 values more accurately than the ANN models in the testing period for all the 7 stations based on

the lower values of the RMSE, RSR, SI, and MAE and higher values of the R and NSE criteria. This proves that the COOT algorithm was successful in determining the optimal weight and bias of the ANN model in all the stations. However, comparing the model's performances at the stations reveals that both the models do not perform satisfactory at Tennant Creek Airport station (e.g., the NSE values are 0.515 and 0.581 for the ANN and COOT-ANN models, respectively). Table 5 shows that the proposed COOT-ANN has detected the best solution with the maximum cost, high accuracy, and less error with substantial progress compared to ANN model.

The scatter and time series plots of the observed and predicted daily ET_0 of the ANN and COOT-ANN models, for all the seven stations, are presented in Figs. 6 and 7. In the scatter plot, a series of dots represents the values of two numerical variables. The horizontal axis represents the values of one variable, while the vertical axis represents the values of the second variable. An analysis of scatter plots is used to examine relationships between variables. Using a scatter plot, the dots indicate not only the values but also patterns that can be observed based on the data. A trend line was added to the scatter plot to display the mathematically best fit to the data when analyzing predictive or correlational relationships between variables. Dots with a clearly clustered pattern, or those that follow a curve or trend line closely, are considered to have a strong relationship. A time

Fig. 4 Pseudo code of the COOT bird natural life model

Pseudo Code of COOT Optimization Algorithm	
Initialize the first population of Coots	
Initialize the parameters of P, Number of Leaders, and Number of Coots	
Random selection of leaders from the Coots	
Calculate the fitness function based on Coots and leaders	
Select the best cost function (Coot or leader) as the global optimum (G_Best)	
while the end criterion	
Calculate A, B parameters	
if rand < P	
R, R1 and R3 are random vectors along the dimensions of the problem.	
Else	
R, R1 and R3 are random number	
For I = 1 to the number of the Coots	
Calculate the parameter of K	
If rand > 0.5	
Update the Coot's positions	
Else	
If rand < 0.5 I ~ 1	
Update the Coot's positions	
Else	
Update the Coot's positions	
Calculate the cost fitness of Coot	
If Coot's fitness < leader's (k) fitness	
leader(k), Coot = Coot, leader(k)	
For number of Leaders	
If rand < 0.5	
Update the position of the Leader	
Else	
Update the position of the Leader	
If the fitness of leader < G_Best	
G_Best, leader = leader, G_Best (Update Global optimum)	
Iteration = Iteration + 1	

Table 4 Model performance based on NSE and RSR criteria

Criterion	Performance	Criterion	Performance
NSE		RSR	
$0.75 \leq NSE \leq 1.00$	Very good	$0.00 \leq RSR \leq 0.50$	Very good
$0.65 \leq NSE \leq 0.75$	Good	$0.50 \leq RSR \leq 0.60$	Good
$0.50 \leq NSE \leq 0.65$	Satisfactory	$0.60 \leq RSR \leq 0.70$	Satisfactory
$NSE \leq 0.50$	Unsatisfactory	$RSR \leq 0.70$	Unsatisfactory

series plot is useful for determining how the data has trended over time as well as if the data points are random or show any patterns over time. The time series plot is also useful for comparing the results of different models. In analyzing the results of the time series graph, the lower error shows that the observed values are well predicted by the model and there are the fewer outlier's data. Comparing the time series plots of these two figures indicates that in overall, the COOT-ANN model is significantly more accurate than the

ANN model in estimating ET_0 , especially the extreme (minimum and maximum) values in all stations (except the Tennant Creek Airport station at which both of the models do not show satisfactory performance). Also, according to the scatter plots, the predicted data of the COOT-ANN model (Leinster Aero station ($R^2 = 0.819$), Charleville Aero ($R^2 = 0.825$), Stawell Aerodrome ($R^2 = 0.828$), Tennant Creek Airport ($R^2 = 0.594$), Woomera Aerodrome ($R^2 = 0.862$), Butlers Gorge ($R^2 = 0.715$), and Mudgee Airport ($R^2 = 0.813$)) have higher R^2 values, and show less scatter than those of the ANN values (Leinster Aero station ($R^2 = 0.806$), Charleville Aero ($R^2 = 0.815$), Stawell Aerodrome ($R^2 = 0.817$), Tennant Creek Airport ($R^2 = 0.575$), Woomera Aerodrome ($R^2 = 0.855$), Butlers Gorge ($R^2 = 0.705$), and Mudgee Airport ($R^2 = 0.798$)) (Figs. 6 and 7).

In Fig. 8, the Taylor diagram can be used to compare the models. In the next step, the ANN and COOT-ANN models were compared with each other using the Taylor diagrams (Taylor 2001) in the testing phase (Fig. 8). As can be seen in the Taylor diagram, it is possible to visualize how closely model estimations match the observations (Taylor 2001). In

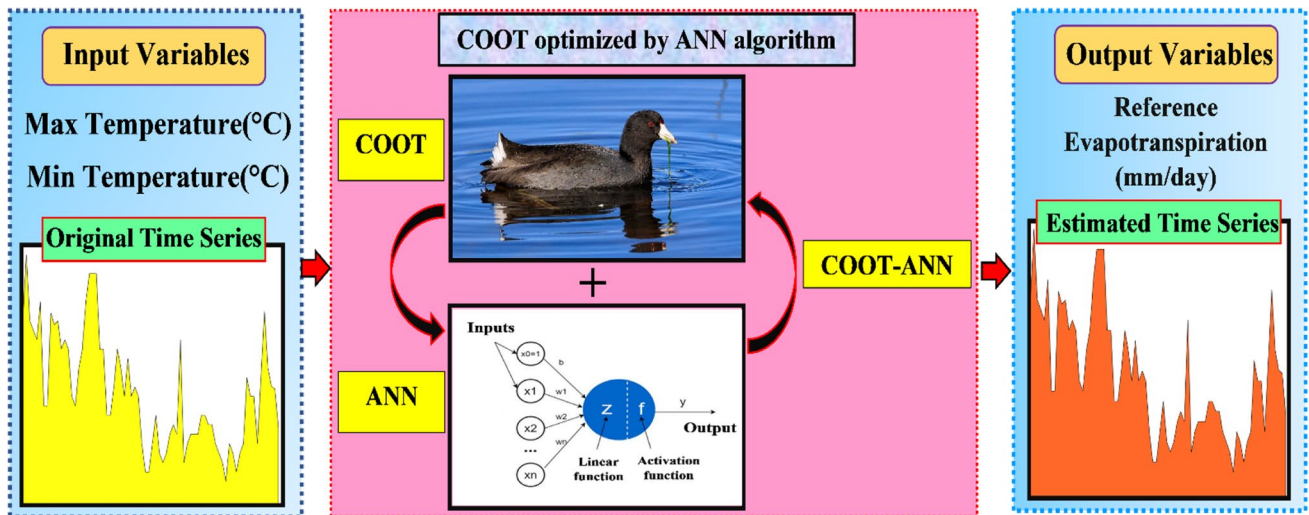


Fig. 5 Schematic diagram of the proposed methodology

Table 5 Performance metrics of the models in the training and testing process for ANN and COOT-ANN modes

Site	ANN											
	Training						Testing					
	R	RMSE (mm/day)	NSE	RSR	SI	MAE	R	RMSE (mm/day)	NSE	RSR	SI	MAE
Leinster Aero	0.910	1.252	0.828	0.415	0.202	0.982	0.898	1.254	0.804	0.443	0.189	0.992
Charleville Aero	0.904	1.100	0.818	0.427	0.199	0.846	0.903	1.090	0.805	0.441	0.185	0.837
Stawell Aerodrome	0.904	1.042	0.817	0.427	0.281	0.821	0.904	0.983	0.814	0.432	0.274	0.763
Tennant Creek Airport	0.768	1.347	0.590	0.641	0.183	1.060	0.759	1.513	0.515	0.697	0.182	1.170
Woomera Aerodrome	0.919	1.307	0.844	0.395	0.206	1.014	0.925	1.199	0.852	0.384	0.186	0.925
Butlers Gorge	0.837	0.824	0.701	0.547	0.397	0.654	0.840	0.765	0.703	0.545	0.371	0.614
Mudgee Airport	0.887	1.008	0.788	0.461	0.258	0.795	0.894	1.014	0.795	0.452	0.262	0.790
	COOT-ANN											
Leinster Aero	0.911	1.243	0.830	0.412	0.200	0.988	0.905	1.205	0.819	0.426	0.182	0.976
Charleville Aero	0.904	1.107	0.816	0.429	0.200	0.856	0.908	1.040	0.823	0.421	0.176	0.803
Stawell Aerodrome	0.907	1.029	0.822	0.422	0.278	0.800	0.910	0.944	0.828	0.415	0.263	0.731
Tennant Creek Airport	0.768	1.370	0.575	0.652	0.186	1.091	0.771	1.406	0.581	0.648	0.169	1.102
Woomera Aerodrome	0.919	1.306	0.844	0.395	0.206	1.020	0.929	1.160	0.862	0.372	0.180	0.901
Butlers Gorge	0.840	0.819	0.705	0.543	0.394	0.651	0.846	0.750	0.714	0.535	0.364	0.599
Mudgee Airport	0.890	0.999	0.792	0.457	0.256	0.778	0.902	0.972	0.812	0.433	0.251	0.751

The blue and gray cells show the identical and high ability of the models, respectively

a Taylor diagram, standard deviation (SD), root mean square deviation (RMSD), and correlation coefficient (R) are summarized in one diagram suitable for illustrating the effectiveness of predictive tools based on polar diagram. As the azimuth angle represents the coefficient of correlation, the radial location from the beginning represents the standard deviation proportion. Each model is measured by its distance from the observed point along the horizontal axis. The distance

between a model and the observed point is a measure of its accuracy. Due to this, the closest point to the observed point performs the best. The Taylor diagram (Fig. 8) shows the prediction made by COOT-ANN algorithm and ANN model at all seven stations, where the red contours are representative of correlation coefficients, blue contours are representative of RMSD errors, and black contours are indicative of standard deviations. Figure 8 illustrates that the COOT-ANN

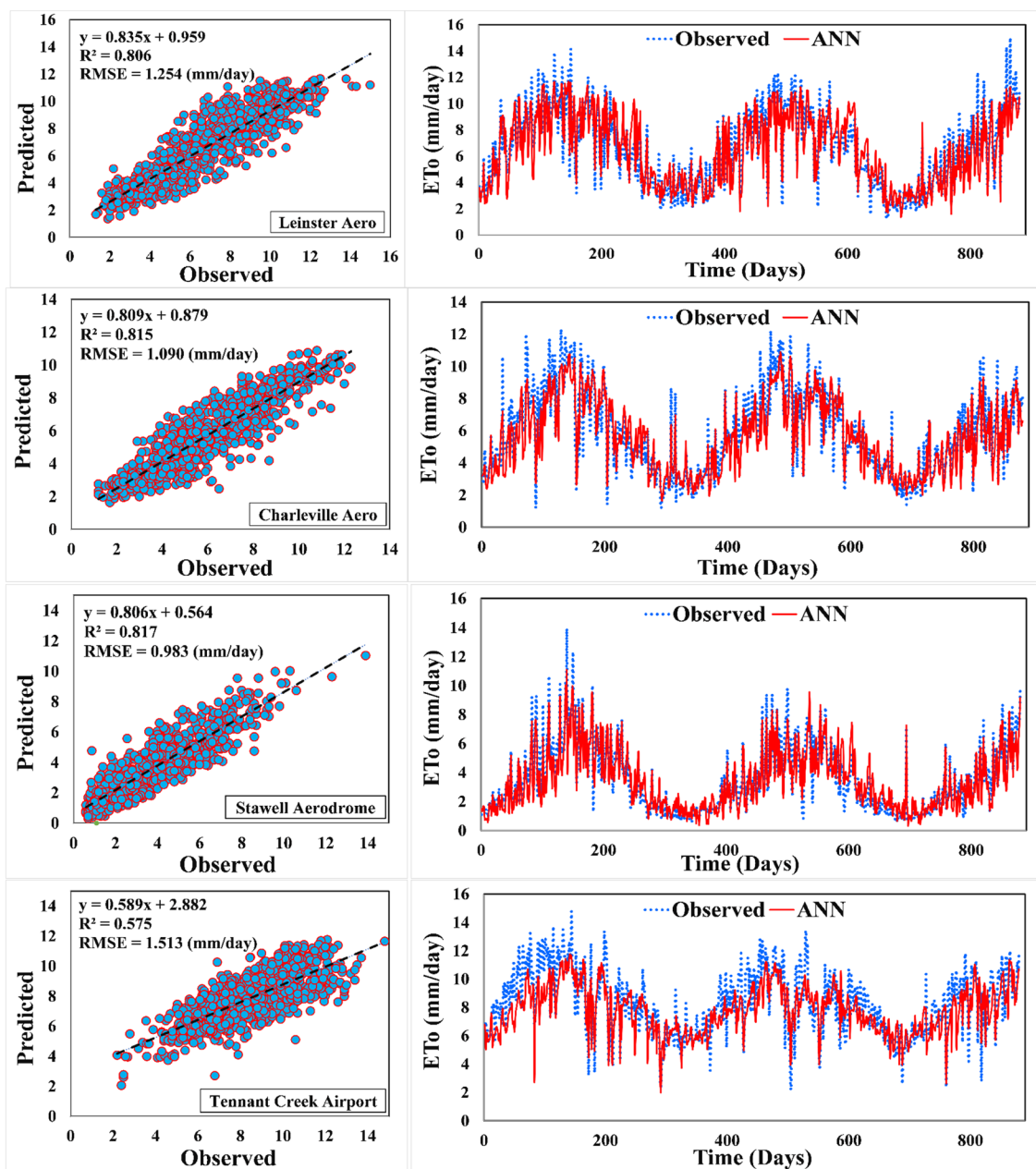


Fig. 6 Scatter and time series plots of the ANN model during the testing phase

models are more accurate and higher performance than the ANN based on the distance of the COOT-ANN point from the observed point for all stations ((Leinster Aero station ($R_{ANN} = 0.898$, $R_{COOT-ANN} = 0.905$; $RMSE_{ANN} = 1.254$, $RMSE_{COOT-ANN} = 1.205$), Charleville Aero ($R_{ANN} = 0.903$, $R_{COOT-ANN} = 0.908$; $RMSE_{ANN} = 1.090$, $RMSE_{COOT-ANN} = 1.040$), Stawell Aerodrome ($R_{ANN} = 0.904$, $R_{COOT-ANN} = 0.910$; $RMSE_{ANN} = 0.983$, $RMSE_{COOT-ANN} = 0.944$), Tennant Creek Airport ($R_{ANN} = 0.759$, $R_{COOT-ANN} = 0.771$; $RMSE_{ANN} = 1.513$, $RMSE_{COOT-ANN} = 1.406$), Woomera Aerodrome ($R_{ANN} = 0.925$, $R_{COOT-ANN} = 0.929$; $RMSE_{ANN} = 1.199$,

$RMSE_{COOT-ANN} = 1.160$), Butlers Gorge ($R_{ANN} = 0.840$, $R_{COOT-ANN} = 0.846$; $RMSE_{ANN} = 0.765$, $RMSE_{COOT-ANN} = 0.750$), Mudgee Airport ($R_{ANN} = 0.894$, $R_{COOT-ANN} = 0.902$; $RMSE_{ANN} = 1.014$, $RMSE_{COOT-ANN} = 0.972$)).

4 Discussion

The results of hybrid and standalone models for simulating ET_o (Table 5) indicated that the hybrid COOT-ANN model performed more successfully than the ANN models

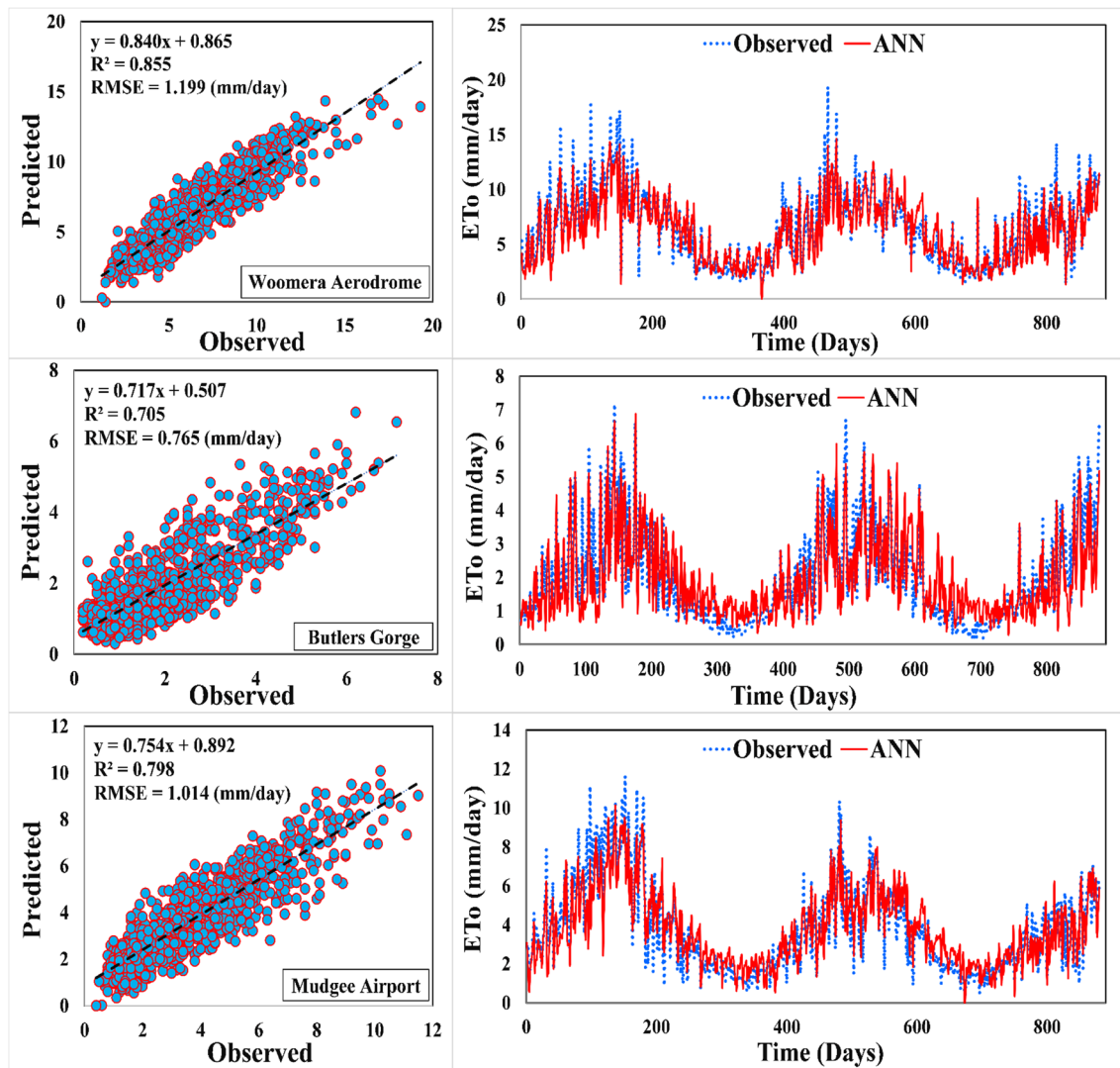


Fig. 6 (continued)

using only the T_{\max} and T_{\min} input variables. Moreover, the statistical indices (including correlation coefficient (R), root mean square error (RMSE), Nash–Sutcliffe efficiency (NSE), RMSE-observation standard deviation ratio (RSR), Scatter Index (SI), and mean absolute error (MAE)) along with the Taylor diagrams are used to determine whether there are significant differences between COOT-ANN and ANN models in a statistical sense. This is in accordance with other similar studies by Silva et al. (2020), Adnan et al. (2021), and Sabzevari and Eslamian (2022). The current study indicates that the hybrid model produced a very promising and encouraging results. The performance criteria indicated that the R criterion of the hybrid model increased by up to 0.803%, the RMSE reduced by up to 4.127%, the NSE increased by up to 3.359%, the RSR reduced by up to 4.072%, the SI reduced by up to 4.148%, and the MAE reduced by up to 3.665% compared

to the ANN model at the testing period. Overall, based on the statistical and visual measures, it is found that in this study similar to the other previous studies (e.g., Seifi and Riahi 2020; and Maroufpoor et al. 2020), the hybrid intelligent models outperform the simple standalone models due to the good performance of the heuristic optimization algorithms (i.e., the COOT algorithm in this study). The COOT-ANN algorithm has several advantages over the ANN model, including simplicity, ease of implementation, and few parameters. To the best of our knowledge, no study has applied this algorithm to prediction of daily crop reference evapotranspiration in Australia. The COOT optimization algorithm is primarily designed to solve continuous optimization problems. Therefore, to address discrete optimization problems, such as crop reference evapotranspiration on a daily basis, the COOT-ANN operators and parameters must be modified.

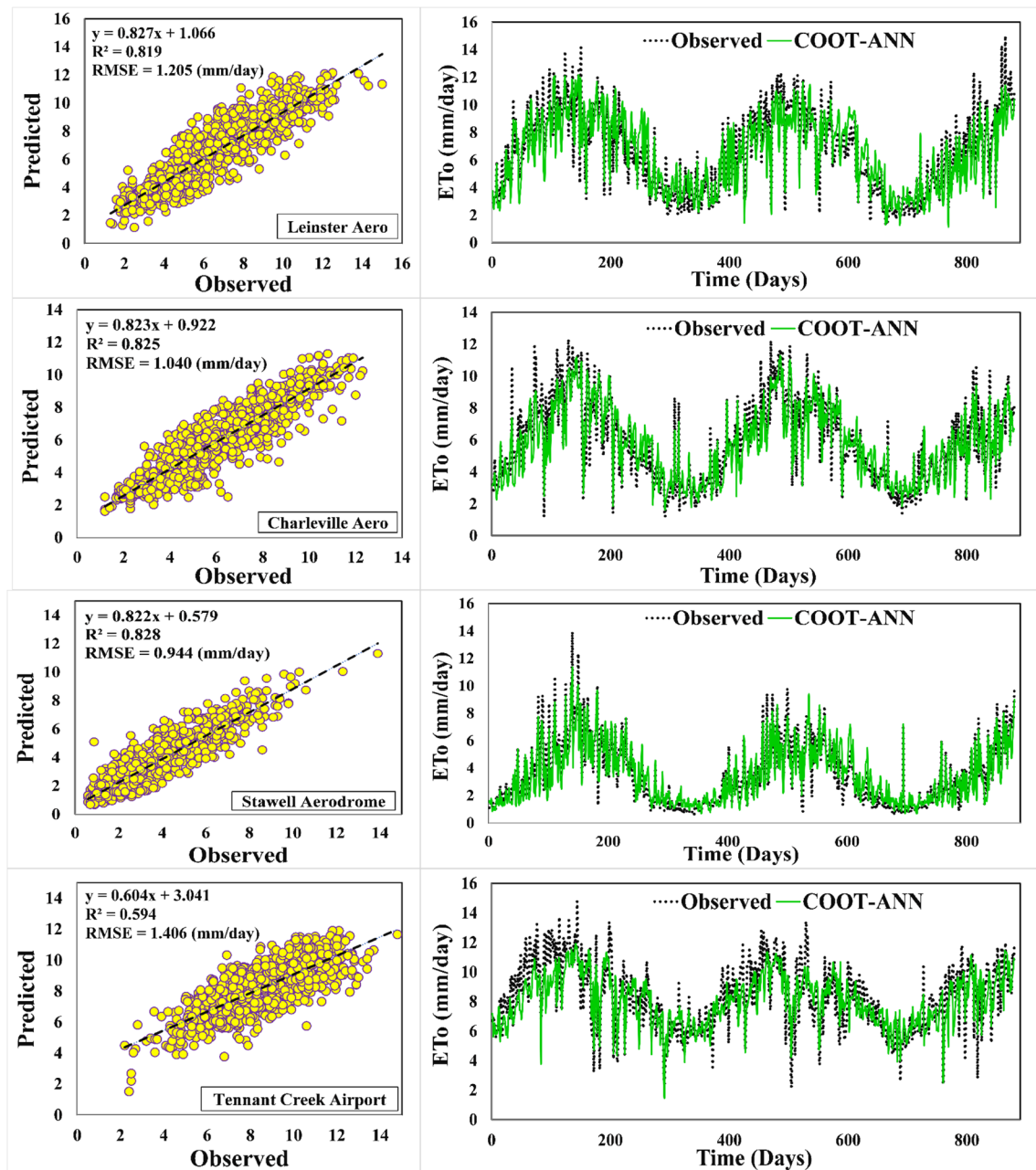


Fig. 7 Scatter and time series plots of the COOT-ANN model during the testing phase

It should be noted that ET_0 processes, like any natural processes, may exhibit both linear and nonlinear behaviors over time. In cases where a time series includes both linear and nonlinear patterns, combining linear and nonlinear models could produce better results. The superior efficiency of this method is achieved by training a black box ensemble method that uses historical observations to learn what weights should be applied to the component parts of the model based on different patterns of historical observations.

There have been very few studies conducted in Australia on prediction of evapotranspiration, which rely primarily

on simple artificial intelligence models (machine learning) or numerical methods related to meteorology (Falamarzi et al. 2014; Perera et al. 2014). But in the present study, a novel hybrid machine learning model (COOT-ANN) was employed to determine the accuracy of the hybrid model compared with the simple model (ANN). One research gap which has been studied in this research was comparison of the results of a simple machine learning model with a completely new and developed hybrid model. In previous studies, they mainly used a lot of weather input variables to predict evapotranspiration, while in this research, only

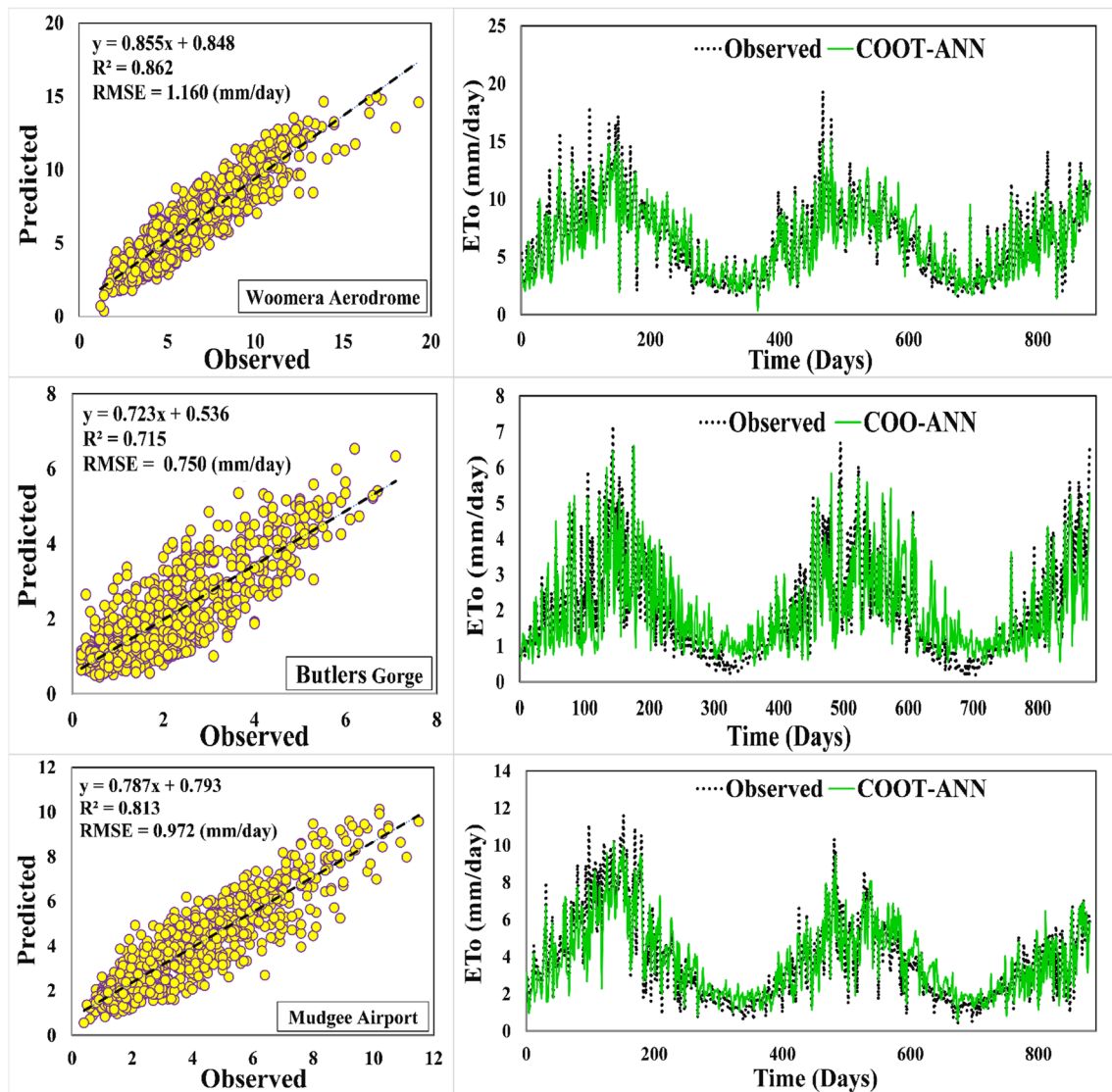


Fig. 7 (continued)

two input variables (T_{\max} and T_{\min}) were used to predict crop reference evapotranspiration in this research, the basic COOT and ANN algorithms were successfully combined to develop a novel hybrid meta-heuristic algorithm (COOT-ANN) with better all-around search performance for global optimization. To assess the performance of the developed COOT-ANN algorithm, the maximum iteration, population size, and learning rate were set as 1000, 500, and 0.001, respectively. Experimental results demonstrated that COOT-ANN performs better than pure model solution accuracy, convergence speed, stability, and local optima avoidance.

The accuracy of the applied ANN-based models differs significantly at the different selected sites based on two factors of statistical characteristics (such as the skewness, kurtosis, coefficient of variation, and average) of the training data and then the generated weights of the models in various

sites. To achieve the best results from the hybrid models, it is important that the input data have lower skewness, kurtosis, coefficient of variation, and higher mean value (Rajae and Shahabi 2015; Kisi 2005).

5 Conclusion

One of the most important components of the hydrological cycle is crop reference evapotranspiration. A wide range of the hydrological and water resource processes are affected by crop reference evapotranspiration. It is therefore imperative to quantify this process for the sustainable management of water resources. The Penman–Monteith method is a standard method for estimating the crop reference evapotranspiration, ET_0 (Allen et al. 1998); however, this model is not capable of estimating

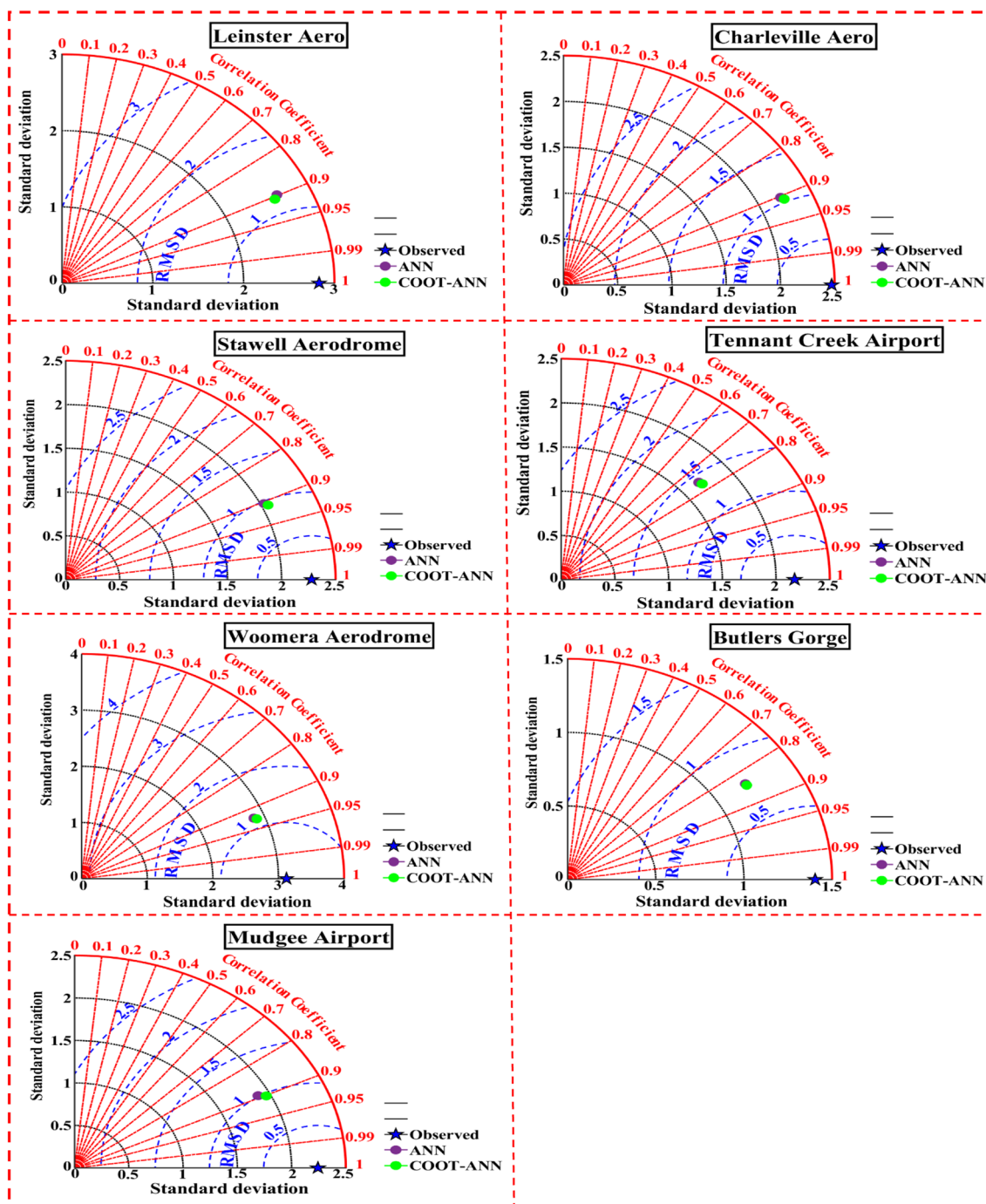


Fig. 8 Taylor diagrams of the models in the testing period for seven stations

the ET_0 in regions with limited meteorological data as the method requires a large number of variables. In this study, a new optimization algorithm, i.e., COOT bird natural life algorithm hybridized with the artificial neural network (COOT-ANN model) was developed and evaluated for the prediction of daily ET_0 using just two meteorological data (T_{max} and T_{min}) from seven stations in different states of Australia. The COOT-ANN model was compared with the classical ANN model

using statistical indices such as correlation coefficient (R), root-mean-squared error (RMSE), Nash–Sutcliffe efficiency (NSE), RMSE-observation standard deviation ratio (RSR), Scatter Index (SI), mean absolute error (MAE), and Taylor diagrams. Several factors are important in the development of new algorithms, including accuracy enhancements, error reductions, model simplicity, ease of model development, run time reduction, and less computations. Researchers from all over the world

continuously introduce more new optimizer models, which are inspired by a variety of topics and sources. However, the new algorithms are not able to optimize the coefficients of the artificial neural network models and are largely trapped in their local optimal points. Therefore, only a limited number of them can effectively optimize ANN coefficients in comparison to classical methods. The results of this study proved that the COOT-ANN model was more accurate and efficient than the classical ANN model in estimating daily ET_0 at all seven stations. It is recommended that the COOT-ANN model to be applied and evaluated in modeling other hydrological variables in Australia and other parts of the world. Moreover, since only seven sites were selected in this study, it is recommended that the validity of the developed hybrid model to be investigated in different locations with different agro-climatic conditions. Also, hybridization of the COOT algorithm with other intelligent standalone techniques and examining the developed models in prediction problems is recommended. However, a significant portion of future research can be devoted to minimizing uncertainties and improving optimization performance.

Author contributions Ehsan Mirzania and Mohsen Saroughi: conceived the problem, data collection, and designed the analysis. Mahsa Hasanpour Kashani and Ehsan Mirzania: prepared draft and graphical design. Osama Ragab Ibrahim and Mohsen Saroughi: contributed data and analysis tools and writing review and editing. Mohsen Saroughi and Ehsan Mirzania: Coding and Runing. Golmar Golmohammadi: supervision. All authors read and approved the final manuscript.

Data availability The datasets, analyzed during the current study, were compiled and supplied from the Australian Meteorological Agency (BOM) (<http://www.bom.gov.au>). They are available from the corresponding author on reasonable request.

Declarations

Conflict of interest The authors declare no competing interests.

References

- Abrishami N, Sepaskhah AR, Shahrokhnia MH (2019) Estimating wheat and maize daily evapotranspiration using artificial neural network. *Theor Appl Climatol* 135:945–958. <https://doi.org/10.1007/s00704-018-2418-4>
- Achite M, Jehanzaib M, Sattari MT, Toubal AK, Elshaboury N, Wałęga A, Krakauer N, Yoo JY, Kim TW (2022) Modern techniques to modeling reference evapotranspiration in a semiarid area based on ANN and GEP models. *Water* 14:1210. <https://doi.org/10.3390/w14081210>
- Adnan RM, Heddami S, Yaseen ZM, Shahid S, Kisi O, Li B (2021) Prediction of potential evapotranspiration using temperature-based heuristic approaches. *Sustainability* 13:297. <https://doi.org/10.3390/su13010297>
- Ahmadi F, Mehdizadeh S, Mohammadi B, Pham QB, Doan TNC, Vo ND (2021) Application of an artificial intelligence technique enhanced with intelligent water drops for monthly reference evapotranspiration estimation. *Agric Water Manag* 244:106622. <https://doi.org/10.1016/j.agwat.2020.106622>
- Ahmed AAM, Deo RC, Feng Q, Ghahramani A, Raj N, Yin Z, Yang L (2022) Hybrid deep learning method for a week-ahead evapotranspiration forecasting. *Stoch Environ Res Risk Assess* 36:831–849. <https://doi.org/10.1007/s00477-021-02078-x>
- Allen RG, Pereira LS, Raes D, Smith M (1998) Crop evapotranspiration-guidelines for computing crop water requirements. In: *FAO Irrigation and Drainage Paper 56*. Food and Agriculture Organization of the United Nations, Rome, Italy
- Antonopoulos VZ, Antonopoulos AV (2017) Daily reference evapotranspiration estimates by artificial neural networks technique and empirical equations using limited input climate variables. *Comput Electron Agric* 132:86–96
- Chen X, Li FW, Wang YX, Feng P, Yang RZ (2019a) Evolution properties between meteorological, agricultural and hydrological droughts and their related driving factors in the Luanhe River basin, China. *Hydrol Res* 50:1096–1119. <https://doi.org/10.2166/nh.2019.141>
- Chen Z, Yang X, Liu X (2019b) RBFNN-based non-singular fast terminal sliding mode control for robotic manipulators including actuator dynamics. *Neurocomputing* 362:72–82. <https://doi.org/10.1016/j.neucom.2019.06.083>
- Chen Z, Zhu Z, Jiang H, Sun S (2020) Estimating daily reference evapotranspiration based on limited meteorological data using deep learning and classical machine learning methods. *J Hydrol* 591. <https://doi.org/10.1016/j.jhydrol.2020.125286>
- Dias SHB, Filgueiras R, Filho EIF, Arcanjo GS, Silva GH, Mantovani EC, Cunha FF (2021) Reference evapotranspiration of Brazil modeled with machine learning techniques and remote sensing. *PLoS ONE* 16(2):e0245834. <https://doi.org/10.1371/journal.pone.0245834>
- Djaman K, O'Neill M, Diop L, Bodian A, Allen S, Koudahe K, Lombard K (2019) Evaluation of the Penman-Monteith and other 34 reference evapotranspiration equations under limited data in a semiarid dry climate. *Theor Appl Climatol* 137(1):729–743. <https://doi.org/10.1007/s00704-018-2624-0>
- Douna V, Barraza V, Grings F, Huete A, Coupe NR, Beringer J (2021) Towards a remote sensing data based evapotranspiration estimation in Northern Australia using a simple random forest approach. *J Arid Environ* 191:104513. <https://doi.org/10.1016/j.jaridenv.2021.104513>
- Elbeltagi A, Kushwaha NL, Rajput J et al (2022) Modelling daily reference evapotranspiration based on stacking hybridization of ANN with meta-heuristic algorithms under diverse agro-climatic conditions. *Stoch Environ Res Risk Assess* 36:3311–3334. <https://doi.org/10.1007/s00477-022-02196-0>
- Exner-Kittridge MG, Rains MC (2010) Case study on the accuracy and cost/effectiveness in simulating reference evapotranspiration in West-Central Florida. *J Hydrol Eng* 15(9):696–703. [https://doi.org/10.1061/\(ASCE\)HE.1943-5584.0000239](https://doi.org/10.1061/(ASCE)HE.1943-5584.0000239)
- Falamarzi Y, Palizdan N, Huang YF, Lee TS (2014) Estimating evapotranspiration from temperature and wind speed data using artificial and wavelet neural networks (WNNs). *Agric Water Manage* 140:26–36. <https://doi.org/10.1016/j.agwat.2014.03.014>
- Fan J, Yue W, Wu L, Zhang F, Cai H, Wang X, Lu X, Xiang Y (2018) Evaluation of SVM, ELM and four tree-based ensemble models for predicting daily reference evapotranspiration using limited meteorological data in different climates of China. *Agric For Meteorol* 263:225–241. <https://doi.org/10.1016/j.agrformet.2018.08.019>
- Farias DBS, Althoff D, Rodrigues LN, Filgueiras R (2020) Performance evaluation of numerical and machine learning methods in estimating reference evapotranspiration in a Brazilian agricultural frontier. *Theor Appl Climatol* 142:1481–1492. <https://doi.org/10.1007/s00704-020-03380-4>

- Feng Y, Gong D, Mei X, Cui N (2017) Estimation of maize evapotranspiration using extreme learning machine and generalized regression neural network on the China Loess Plateau. *Hydrol Res* 48(4):1156–1168. <https://doi.org/10.2166/nh.2016.099>
- Ferreira LB, Cunha FFD, Oliveira RAD, Filho EIF (2019) Estimation of reference evapotranspiration in Brazil with limited meteorological data using ANN and SVM—A new approach. *J Hydrol* 572:556–570. <https://doi.org/10.1016/j.jhydrol.2019.03.028>
- Gao L, Gong D, Cui N, Lv M, Feng Y (2021) Evaluation of bio-inspired optimization algorithms hybrid with artificial neural network for reference crop evapotranspiration estimation. *Comput Electron Agric* 190:106466. <https://doi.org/10.1016/j.compag.2021.106466>
- Gocić M, Amiri MA (2021) Reference evapotranspiration prediction using neural networks and optimum time lags. *Water Resour Manage* 35:1913–1926. <https://doi.org/10.1007/s11269-021-02820-8>
- Hashemi M, Sepaskhah AR (2020) Evaluation of artificial neural network and Penman–Monteith equation for the prediction of barley standard evapotranspiration in a semi-arid region. *Theor Appl Climatol* 139:275–285. <https://doi.org/10.1007/s00704-019-02966-x>
- Huang G, Wu L, Ma X, Zhang W, Fan J, Yu X, Zeng W, Zhou H (2019) Evaluation of CatBoost method for prediction of reference evapotranspiration in humid regions. *J Hydrol* 574:1029–1041. <https://doi.org/10.1016/j.jhydrol.2019.04.085>
- Kaya YZ, Zelenakova M, Ůneš F, Demirci M, Hlavata H, Mesáros P (2021) Estimation of daily evapotranspiration in Košice City (Slovakia) using several soft computing techniques. *Theor Appl Climatol* 144:287–298. <https://doi.org/10.1007/s00704-021-03525-z>
- Keshtegar B, Abdullah SS, Huang YF et al (2022) Reference evapotranspiration prediction using high-order response surface method. *Theor Appl Climatol* 148:849–867. <https://doi.org/10.1007/s00704-022-03954-4>
- Kisi O (2005) Suspended sediment estimation using neurofuzzy and neural network approaches. *Hydrol Sci J* 50(4):683–696
- Kisi O, Keshtegar B, Zounemat-Kermani M, Heddami S, Trung NT (2021) Modeling reference evapotranspiration using a novel regression-based method: radial basis M5 model tree. *Theor Appl Climatol* 145:639–659. <https://doi.org/10.1007/s00704-021-03645-6>
- Koudahe K, Djaman K, Adewumi JK (2018) Evaluation of the Penman–Monteith reference evapotranspiration under limited data and its sensitivity to key climatic variables under humid and semiarid conditions. *Model Earth Syst Environ* 4(3):1239–1257. <https://doi.org/10.1007/s40808-018-0497-y>
- Majhi B, Naidu D (2021) Differential evolution based radial basis function neural network model for reference evapotranspiration estimation. *SN Appl Sci* 3(1):1–19. <https://doi.org/10.1007/s42452-020-04069-z>
- Majumdar P, Bhattacharya D, Mitra S (2023) Prediction of evapotranspiration and soil moisture in different rice growth stages through improved salp swarm based feature optimization and ensemble machine learning algorithm. *Theor Appl Climatol*. <https://doi.org/10.1007/s00704-023-04414-3>
- Maroufpoor S, Bozorg-Haddad O, Maroufpoor E (2020) Reference evapotranspiration estimating based on optimal input combination and hybrid artificial intelligent model: hybridization of artificial neural network with grey wolf optimizer algorithm. *J Hydrol* 588. <https://doi.org/10.1016/j.jhydrol.2020.125060>
- Mawgoud AH, Fathy A, Kamel S (2022) An effective hybrid approach based on arithmetic optimization algorithm and sine cosine algorithm for integrating battery energy storage system into distribution networks. *J Energy Storage* 49:104154. <https://doi.org/10.1016/j.est.2022.104154>
- Mirzania E, Vishwakarma DK, Bui QAT et al (2023) A novel hybrid AIG-SVR model for estimating daily reference evapotranspiration. *Arab J Geosci* 16:301. <https://doi.org/10.1007/s12517-023-11387-0>
- Mohammadi B, Linh NTT, Pham QB, Ahmed AN, Vojteková J, Guan Y, Abba SI, El-Shafie A (2020) Adaptive neuro-fuzzy inference system coupled with shuffled frog leaping algorithm for predicting river streamflow time series. *Hydrol Sci J* 65:1738–1751. <https://doi.org/10.1080/02626667.2020.1758703>
- Mokari E, DuBois D, Samani Z, Mohebzadeh H, Djaman K (2021) Estimation of daily reference evapotranspiration with limited climatic data using machine learning approaches across different climate zones in New Mexico. *Theor Appl Clim* 147:575–587. <https://doi.org/10.1007/s00704-021-03855-y>
- Mostafa RR, Hussien AG, Khan MA, Kadry S, Hashim FA (2022) Enhanced COOT optimization algorithm for Dimensionality Reduction. 2022 Fifth Int Conf Women Data Sci Prince Sultan Univ (WiDS PSU):43–48. <https://doi.org/10.1109/WiDS-PSU54548.2022.00020>
- Muhammad MKI, Shahid S, Ismail T, Harun S, Kisi O, Yaseen ZM (2021) The development of evolutionary computing model for simulating reference evapotranspiration over Peninsular Malaysia. *Theor Appl Climatol* 144:1419–1434. <https://doi.org/10.1007/s00704-021-03606-z>
- Naruei I, Keynia F (2021) A new optimization method based on COOT Bird Natural Life Model. *Expert Syst Appl* 183:115352. <https://doi.org/10.1016/j.eswa.2021.115352>
- Nawandar NK, Cheggoju N, Satpute V (2021) ANN-based model to predict reference evapotranspiration for irrigation estimation. In: Gunjan VK, Zurada JM (eds) Proceedings of International Conference on Recent Trends in Machine Learning, IoT, Smart Cities and Applications. Advances in Intelligent Systems and Computing, vol 1245. Springer, Singapore. https://doi.org/10.1007/978-981-15-7234-0_63
- Niaghi AR, Hassanjalilian O, Shiri J (2021) Estimation of reference evapotranspiration using spatial and temporal machine learning approaches. *Hydrology* 8:25. <https://doi.org/10.3390/hydrology8010025>
- Nourani V (2017) An emotional ANN (EANN) approach to modeling rainfall-runoff process. *J Hydrol* 544:267–277. <https://doi.org/10.1016/j.jhydrol.2016.11.033>
- Nourani V, Elkiran G, Abdullahi J (2019) Multi-station artificial intelligence based ensemble modeling of reference evapotranspiration using pan evaporation measurements. *J Hydrol* 577:123958. <https://doi.org/10.1016/j.jhydrol.2019.123958>
- Perera KC, Western AW, Nawarathna B, George B (2014) Forecasting daily reference evapotranspiration for Australia using numerical weather prediction outputs. *Agric For Meteorol* 194:50–63. <https://doi.org/10.1016/j.agrformet.2014.03.014>
- Pour SH, Wahab AKA, Shahid S, Wang X (2019) Spatial pattern of the unidirectional trends in thermal bioclimatic indicators in Iran. *Sustainability* 11:2287. <https://doi.org/10.3390/su11082287>
- Rajaei T, Shahabi A (2015) Evaluation of wavelet-GEP and wavelet-ANN hybrid models for prediction of total nitrogen concentration in coastal marine waters. *Arab J Geosci* 9:176
- Sabzevari Y, Eslamian S (2022) Predicting the effect of temperature changes on reference evapotranspiration by means of time series modeling (case study: Khorramabad Basin). *Irrig Sci Eng* 45(2):125–138. <https://doi.org/10.22055/jise.2022.40355.2022>
- Salman SA, Shahid S, Ismail T, Chung ES, Al-Abadi AM (2017) Longterm trends in daily temperature extremes in Iraq. *Atmos Res* 198:97–107. <https://doi.org/10.1016/j.atmosres.2017.08.011>
- Seifi A, Riahi H (2020) Estimating daily reference evapotranspiration using hybrid gamma test-least square support vector machine, gamma test-ANN, and gamma test-ANFIS models in an arid area of Iran. *J Water Clim Change* 11(1):217–240. <https://doi.org/10.2166/wcc.2018.003>

- Sharafi S, Ghalehi MM (2021) Evaluation of multivariate linear regression for reference evapotranspiration modeling in different climates of Iran. *Theor Appl Climatol* 143(3):1409–1423. <https://doi.org/10.1007/s00704-020-03473-0>
- Shiri J (2017) Evaluation of FAO56-PM, empirical, semi-empirical and gene expression programming approaches for estimating daily reference evapotranspiration in hyper-arid regions of Iran. *Agric Water Manag* 188:101–114. <https://doi.org/10.1016/j.agwat.2017.04.009>
- Silva CRD, Barbosa LA, Finzi RR, Riberio BT, Dias NDS (2020) Accuracy of air temperature forecasts and its use for prediction of the reference evapotranspiration. *Biosci J* 36:17–22. <https://doi.org/10.14393/BJ-v36n1a2020-42188>
- Taylor KE (2001) Summarizing multiple aspects of model performance in a single diagram. *J Geophys Res Atmos* 106:7183–7192. <https://doi.org/10.1029/2000JD900719>
- Üneş F, Kaya YZ, Mamak M (2020) Daily reference evapotranspiration prediction based on climatic conditions applying different data mining techniques and empirical equations. *Theor Appl Climatol* 141(1–2):763–773. <https://doi.org/10.1007/s00704-020-03225-0>
- Valiantzas JD (2015) Simplified limited data Penman's ET0 formulas adapted for humid locations. *J Hydrol* 524:701–707. <https://doi.org/10.1016/j.jhydrol.2015.03.021>
- Yamaç SS, Todorovic M (2020) Estimation of daily potato crop evapotranspiration using three different machine learning algorithms and four scenarios of available meteorological data. *Agric Water Manag* 228:105875. <https://doi.org/10.1016/j.agwat.2019.105875>
- Yang Q, Wang JQ, Hakala K (2022) Calibrating anomalies improves forecasting of daily reference crop evapotranspiration. *J Hydrol* 610. <https://doi.org/10.1016/j.jhydrol.2022.128009>
- Yu H, Wen X, Li B, Yang Z, Wu M, Ma Y (2020) Uncertainty analysis of artificial intelligence modeling daily reference evapotranspiration in the northwest end of China. *Comput Electron Agric* 176:105653. <https://doi.org/10.1016/j.compag.2020.105653>
- Zhao T, Wang QJ, Schepen A, Griffiths M (2019) Ensemble forecasting of monthly and seasonal reference crop evapotranspiration based on global climate model outputs. *Agric Meteorol* 264:114–124. <https://doi.org/10.1016/j.agrformet.2018.10.001>

Publisher's note Springer Nature remains neutral with regard to jurisdictional claims in published maps and institutional affiliations.

Springer Nature or its licensor (e.g. a society or other partner) holds exclusive rights to this article under a publishing agreement with the author(s) or other rightsholder(s); author self-archiving of the accepted manuscript version of this article is solely governed by the terms of such publishing agreement and applicable law.